Numerical Study of Natural Convection in an Inclined Triangular Cavity for Different Thermal Boundary Conditions: Application of the Lattice Boltzmann Method

Ahmed Mahmoudi[1,2]**, Imen Mejri**[1]**, Mohamed Ammar Abbassi**[1] **and Ahmed Omri**[1]

Abstract: A double-population Lattice Boltzmann Method (LBM) is applied to solve the steady-state laminar natural convective heat-transfer problem in a triangular cavity filled with air ($Pr = 0.71$). Two different boundary conditions are implemented for the vertical and inclined boundaries: Case I) adiabatic vertical wall and inclined isothermal wall, Case II) isothermal vertical wall and adiabatic inclined wall. The bottom wall is assumed to be at a constant temperature (isothermal) for both cases. The buoyancy effect is modeled in the framework of the well-known Boussinesq approximation. The velocity and temperature fields are determined by a D2Q9 LBM and a D2Q4 LBM, respectively. Comparison with previously published work shows excellent agreement. Numerical results are obtained for a wide range of parameters: the Rayleigh number spanning the range $\left(10^3 - 10^6\right)$ and the inclination angle varying in the intervals (0˚ to 120˚) and (0˚ to 360˚) for cases I and II, respectively. Flow and thermal fields are given in terms of streamlines and isotherms distributions. It is observed that inclination angle can be used as a relevant parameter to control heat transfer in right-angled triangular enclosures.

Keywords: Lattice Boltzmann Method, Natural convection, Heat transfer, Right-angled triangular enclosure.

Nomenclature

c	Lattice speed, ms^{-1}
c_s	Speed of sound, ms^{-1}
$\mathbf{c}_i$	Discrete particle speeds, ms^{-1}
F	External forces, kg m s^{-2}

[1] UR:Unité de Recherche Matériaux, Energie et Energies Renouvelables (MEER), Faculté des Sciences de Gafsa, B.P.19, Zarroug, Gafsa, 2112, Tunisie.
[2] Corresponding Author. Email: ahmed.mahmoudi@yahoo.fr; Phone: 00216 97953081

f	Density distribution functions , kg m^{-3}	
f^{eq}	Equilibrium density distribution functions, kg m^{-3}	
g	Internal energy distribution functions, K	
g^{eq}	Equilibrium internal energy distribution functions, K	
$\vec{g}$	Gravity vector , m s^{-2}	
n	Normal direction of the inclined wall	
Ma	Mach number	
Nu	Local Nusselt number	
Pr	Prandtl number	
Ra	Rayleigh number	
T	Temperature, K	
$\mathbf{u}(u,v)$	Velocities , m s^{-1}	
$\mathbf{x}(x,y)$	Lattice coordinates, m	

Greek symbols

Δ	x Lattice spacing, m
Δ	t Time increment, m
τ_{α}	Relaxation time for temperature, s
τ_{v}	Relaxation time for flow, s
v	Kinematic viscosity, m^2 s^{-1}
α	Thermal diffusivity , m^2 s^{-1}
ρ	Fluid density, kg m^{-3}
ψ	Non-dimensional stream function
Φ	Inclination angle
θ	Non-dimensional temperature

Subscript

c	cold
h	hot

1   Introduction

The Lattice Boltzmann Method (LBM) is emerged as a powerful tool to simulate fluid flow, heat and mass transfer. It has become a novel alternative to conventional Computational Fluid Dynamics (CFD) solvers like Finite Difference Method (FDM), Finite Element Method (FEM) and Finite Volume Method (FVM) for solving the Navier–Stokes Equations (NSE) [Chen and Doolen (1998)]. The advantages

of LBM include simple calculation procedures and easy-implementation boundary conditions. It is well suitable for parallel computation, ease and robust in handling of multiphase flow and can be applied for complex geometries. Moreover when using LBM the coupling between pressure and velocity field is avoided; in conventional classical methods this linkage is handled by algorithms such as SIMPLE, SIMPLER [Patankar (1980)] and others which are CPU time consumers. Another advantage it is that can capture turbulence without any turbulence models [Dixit and Bab]. More details about the LBM can be found in the reference [Higuera, Succi and Benzi (1989); Benzi, Succi and Vergassola (1992); Succi (2001)]. Standard benchmark problems have been simulated by LBM and the results were shown to agree well with the classical CFD solvers [McNamara and Alder (1993)].

Many works dealing with convection in enclosures are restricted to the cases of simple geometry, rectangular, cylindrical or spherical cavities. But the real configurations are complex and varied. Natural convection in triangular enclosures has received increased attention due to its direct relevancy to many engineering applications because of its applications to real life configurations such as thermal insulation of buildings using air gaps, solar energy collectors, furnaces and fire control in buildings. A few studies on natural convection on triangular enclosures filled with a viscous fluid have been carried out by earlier researchers [Ostrach (1988); Catton (1978); Gebhart, Jaluria, Mahajan and Sammakia (1988); De Vahl Davis (1983)]. [Asan and Namli (2001)] presented a computational study of natural convection in an isosceles triangular enclosure with a hot horizontal base and cold inclined walls. They used the stream function-vorticity formulation in conjunction with the volume control integration solution technique. Steady state solutions were obtained for Rayleigh number ranging from 10^3 to 10^6. They showed that the height-base ratio and Rayleigh number have profound effect on temperature and flow field. [Rahman, Billah, Rahman, Kalam and Ahsan (2011)] investigated numerically the behavior of nanofluids in an inclined lid-driven triangular enclosure to gain insight into convective recirculation and flow processes induced by nanofluids. It is observed that solid volume fraction strongly influenced the fluid flow and heat transfer in the enclosure. Moreover, the variation of the average Nusselt number and average fluid temperature in the cavity is linear with the solid volume fraction.[Koca, Oztop and Varol (2007)] analyzed the effect of Prandtl number on natural convection heat transfer and fluid flow in triangular enclosures with localized heating. The governing equations of natural convection are formulated based on a stream function–vorticity approach and solved with the finite-difference method. Bottom wall of triangle is heated partially while inclined wall is maintained at a lower uniform temperature than heated wall while remaining walls are insulated. It is observed that both flow and temperature fields are affected with the changing of

Prandtl number, location of heater and length of heater as well as Rayleigh number. [Omri (2007)] deal with a numerical simulation of natural convection flows in a triangular cavity submitted to a uniform heat flux using the Control Volume Finite Element Method (CVFEM). Their results showed that the flow structure is sensitive to the cover tilt angle. Many recirculation zones can occur in the core cavity and the heat transfer is dependent on the flow structure. [Mahmoudi, Pop and Shahi (2012)] investigated numerically natural convection for a two-dimensional triangular enclosure with partially heated from below and cold inclined wall filled with nanofluid in presence of magnetic field. Governing equations are solved by finite volume method. Flow pattern, isotherms and average Nusselt number are presented for six studied cases that are made by location of heat sources. Their results show in presence of magnetic field flow field is suppressed and heat transfer decreases. Furthermore it is observed that maximum reduction of average Nusselt number in high value of Ha occurs at Ra = 10^6. They also found that the nanoparticles are more effective at Ra = 10^4 where conduction is more pronounced. [Ghasemi and Aminossadati (2010)] presented a numerical study on the mixed convection in a lid-driven triangular enclosure filled with a water-Al_2O_3 nanofluid. A comparison study between two different scenarios of upward and downward left sliding walls is presented. The effects of parameters such as Richardson number, solid volume fraction and the direction of the sliding wall motion on the flow and temperature fields as well as the heat transfer rate are examined. The results show that the addition of Al_2O_3 nanoparticles enhances the heat transfer rate for all values of Richardson number and for each direction of the sliding wall motion. However, the downward sliding wall motion results in a stronger flow circulation within the enclosure and hence, a higher heat transfer rate. [Varol (2011)] studied numerically heat transfer and fluid flow due to natural convection in a porous triangular enclosure with a centered conducting body. The center of the body was located onto the gravity center of the right-angle triangular cavity. The Darcy law model was used to write the governing equations and they were solved using a finite difference method. He concluded that both height and width of the body and thermal conductivity ratio play an important role on heat and fluid flow inside the cavity. [Ching , Oztop, Rahman, Islam and Ahsan (2012)] investigated numerically mixed convection heat and mass transfer in a right triangular enclosure is. The bottom surface of the enclosure is maintained at uniform temperature and concentration that are higher than that of the inclined surface. The study is performed for pertinent parameters such as. The effect of buoyancy ratio, Richardson number and the direction of the sliding wall motion parameters on the flow and temperature fields as well as the heat and mass transfer rate examined. The results show that the increase of buoyancy ratio enhances the heat and mass transfer rate for all values of Richardson number and for each direction of the sliding wall motion. However, the direction of the sliding

wall motion can be a good control parameter for the flow and temperature fields.

[Basak, Anandalakshmi and Gunda (2012)] studied numerically entropy generation due to natural convection in right-angled triangular enclosures of various fluids (Pr = 0.025, 7 and 1000). The maximum value of entropy generation, due to fluid flow, is observed near middle portions of the side walls. The location of this maximum depends on the presence of high velocity gradients. [Oztop, Varol , Koca and Firat(2012)] studied experimentally and numerically, heat transfer in a right angle triangular isosceles cavity, filled with air. The bottom wall of the cavity is hot, the inclined wall is cold and the vertical wall is adiabatic. Numerical study is based on the finite difference method. Results, such as the average Nusselt number on the hot wall are shown experimentally and numerically for different angles and for two values of the Rayleigh number 1.5×10^4 and 1.5×10^5. They showed, experimentally, the effect of Rayleigh number and inclination angle on natural convection in a triangular cavity. [Gurkan & Orhan (2013)] studied experimentally and numerically natural convection in a triangular recess, isosceles and right, filled with water, the bottom wall is hot, the vertical wall is cold and the inclined wall is adiabatic. Numerical solutions are obtained using a CFD commercial software, FLUENT, using the finite volume method. They showed, experimentally, the effect of Rayleigh number on natural convection in a triangular cavity.

In this paper, we apply the LBM to solve the non-linear coupled partial differential equations of flow and temperature fields. In the model the velocity and temperature fields are solved by tow independent Lattice Boltzmann equations which are combined into a coupled equation for whole system. Two different boundary conditions are applied to a right-angled triangular enclosure; adiabatic inclined wall with isothermal cold vertical wall or isothermal cold inclined wall with adiabatic vertical wall, the horizontal wall is maintained hot in the two cases. Numerical results are presented in terms of isotherms, streamlines and average Nusselt numbers. The effects of the Rayleigh number and inclination angle are parametrically investigated for the two studied cases.

2 Mathematical formulation

2.1 Problem statement

The cavity has the shape of an isosceles right-angled triangle. It is heated from a wall, and cooled from the other wall. The third wall is maintained adiabatic. The geometry of the present problem is shown in **Fig. 1**, and the thermal boundary conditions for the two studied cases in this paper are represented in **Table 1**. The walls of the cavity are rigid.

Table 1: Definitions of thermal boundary conditions

wall	Case I	Case II
inclined	T_c	$\frac{\partial T}{\partial n} = 0$
vertical	$\frac{\partial T}{\partial x} = 0$	T_c
bottom	T_h	T_h

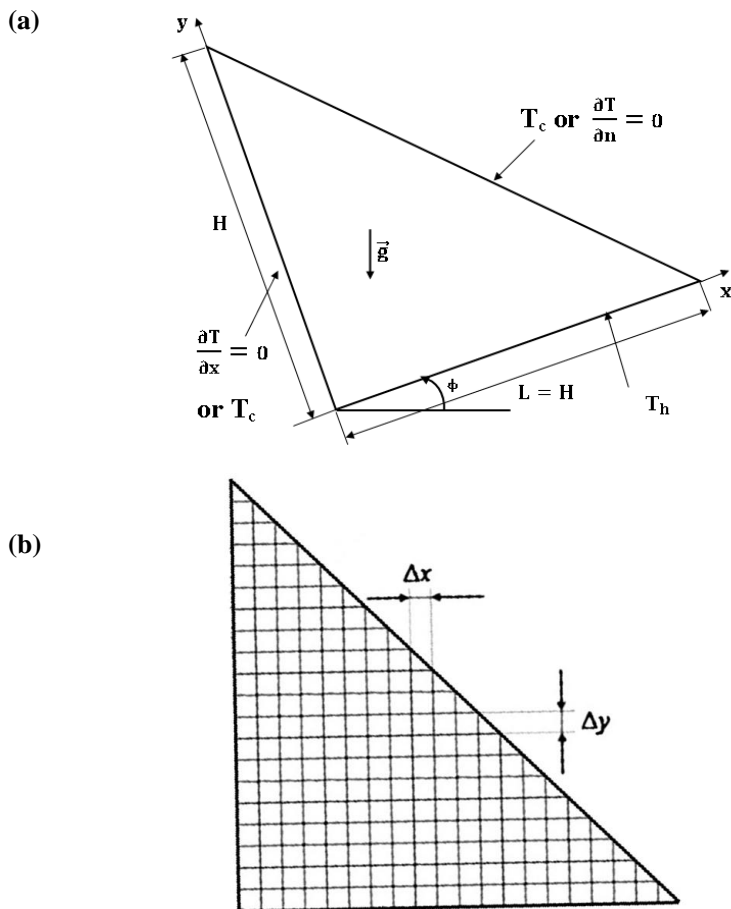Figure 1: (a) Geometry of the present study (b) Grid distribution

For all the walls of the cavity no slip conditions are applied:

$$u = v = 0$$

2.2 Lattice Boltzmann method

For the incompressible non isothermal problems, Lattice Boltzmann Method (LBM) utilizes two distribution functions, f and g, for the flow and temperature fields respectively.

For the flow field:

$$f_i(\mathbf{x} + \mathbf{c_i}\Delta t, t + \Delta t) = f_i(\mathbf{x}, t) - \frac{1}{\tau_v}\left(f_i(\mathbf{x}, t) - f_i^{eq}(\mathbf{x}, t)\right) + \Delta t F_i \tag{1}$$

For the temperature field:

$$g_i(\mathbf{x} + \mathbf{c_i}\Delta t, t + \Delta t) = g_i(\mathbf{x}, t) - \frac{1}{\tau_\alpha}\left(g_i(\mathbf{x}, t) - g_i^{eq}(\mathbf{x}, t)\right) \tag{2}$$

Where the discrete particle velocity vectors defined by $\mathbf{c}_i$, Δt denotes lattice time step which is set to unity. τ_v, τ_α are the relaxation time for the flow and temperature fields, respectively. $f_i^{eq} g_i^{eq}$ are the local equilibrium distribution functions that have an appropriately prescribed functional dependence on the local hydrodynamic properties which are calculated with Eqs.(3) and (4) for flow and temperature fields respectively

$$f_i^{eq} = w_i\rho\left[1 + \frac{3(\mathbf{c_i}.\mathbf{u})}{c^2} + \frac{9(\mathbf{c_i}.\mathbf{u})^2}{2c^4} - \frac{3\mathbf{u}^2}{2c^2}\right] \tag{3}$$

$$g_i^{eq} = w_i'T\left[1 + 3\frac{\mathbf{c_i}.\mathbf{u}}{c^2}\right] \tag{4}$$

$\mathbf{u}$ and ρ are the macroscopic velocity and density, respectively. c is the lattice speed which is equal to $\Delta x/\Delta t$ where Δx is the lattice space similar to the lattice time step Δt which is equal to unity, w_i is the weighting factor for flow, w_i' is the weighting factor for temperature. D2Q9 model for flow and D2Q4 model for temperature are used in this work so that the weighting factors and the discrete particle velocity vectors are different for these two models and they are calculated with Eqs (5-7) as follows:

For D2Q9

$$w_0 = \frac{4}{9}, \ w_i = \frac{1}{9} \ \text{ for } i = 1,2,3,4 \ \text{ and } \ w_i = \frac{1}{36} \ \text{ for } i = 5,6,7,8 \tag{5}$$

$$\mathbf{c_i} = \begin{cases} 0 & i = 0 \\ (\cos\cos[(i-1)\,\pi/2], \sin[(i-1)\pi/2])c & i = 1,2,3,4 \\ \sqrt{2}\,(\cos[(i-5)\,\pi/2 + \pi/4], \sin[(i-5)\pi/2 + \pi/4])\,c & i = 5,6,7,8 \end{cases} \tag{6}$$

For D2Q4

The temperature weighting factor for each direction is equal to $w_i' = 1/4$.

$$\mathbf{c_i} = (\cos\cos[(i-1)\,\pi/2], \sin[(i-1)\pi/2])c \quad i = 1,2,3,4 \tag{7}$$

The kinematic viscosity v and the thermal diffusivity α are then related to the relaxation time by Eq. (8):

$$v = \left[\tau_v - \frac{1}{2}\right] c_s^2 \Delta t \quad \alpha = \left[\tau_\alpha - \frac{1}{2}\right] c_s^2 \Delta t \tag{8}$$

Where c_s is the lattice speed of sound witch is equals to $c_s = c/\sqrt{3}$. In the simulation of natural convection, the external force term F corresponding to the buoyancy force appearing in Eq. (1) is given by Eq.(9)

$$F_i = \frac{\mathbf{G}.(\mathbf{c_i} - \mathbf{u})}{c_s^2} f_i^{\text{eq}} \tag{9}$$

With $\mathbf{G}$ is the external force acting per unit mass. In a natural convection problem it is calculated by the following equation:

$$\mathbf{G} = -\rho\beta\vec{g}\,(T - T_m) \tag{10}$$

Where $\vec{g}$ is the gravitational vector. With the Boussinesq approximation, all the fluid properties are constant except in the body force term where the fluid density varies as

$$\rho = \rho_m\left[1 - \beta(T - T_m)\right] \tag{11}$$

Where ρ_m is the density of the fluid at the mean temperature T_m and β is the thermal expansion coefficient.

The macroscopic quantities, $\mathbf{u}$ and T can be calculated by the mentioned variables, with Eq.(12-14)

$$\rho = \sum_i f_i \tag{12}$$

$$\rho\mathbf{u} = \sum_i f_i \mathbf{c_i} \tag{13}$$

$$T = \sum_i g_i \tag{14}$$

2.3 Non-dimensional parameters

By fixing Rayleigh number, Prandtl number and Mach number the viscosity and thermal diffusivity are calculated from the definition of these non dimensional parameters

$$v = m.Ma.c_s \sqrt{\frac{\text{Pr}}{\text{Ra}}} \tag{15}$$

Where *m* is number of lattices in y-direction. Rayleigh and Prandtl numbers are defined as

$Ra = \frac{\beta g m^3 (T_h - T_c)}{v\alpha}$ and $\text{Pr} = \frac{v}{\alpha}$ respectively. Mach number should be less than $Ma = 0.3$ to insure an incompressible flow. Therefore in the present study, Mach number was fixed at $Ma = 0.1$

Nusselt number is one of the most important dimensionless parameters in the description of the convective heat transport. The local Nusselt number Nu_x and the average value Nu at the hot wall are calculated as:

$$\text{Nu}_x = -\frac{H}{T_h - T_c} \left. \frac{\partial T}{\partial y} \right|_{y=0} \tag{16}$$

$$\text{Nu} = \frac{1}{H} \int_0^H \text{Nu}_x dx \tag{17}$$

2.4 Boundary conditions

The implementation of boundary conditions is very important for the simulation. The distribution functions out of the domain are known from the streaming process. The unknown distribution functions are those toward the domain.

2.4.1 Flow

Bounce-back boundary conditions were applied on all solid boundaries, which means that incoming boundary populations are equal to out-going populations after the collision.

2.4.2 Temperature

The bounce back boundary condition is used on the adiabatic wall. Temperature at the isothermal wall is known. Since we are using D2Q4, the unknown internal energy distribution functions are evaluated respectively as:

Case I

South wall:

$$g_2 = T_H - g_1 - g_3 - g_4 \tag{18}$$

Inclined wall:

$$g_3 = 0.5\left(T_C - g_1 - g_2\right) \quad g_4 = 0.5\left(T_C - g_1 - g_2\right) \tag{19}$$

Case II

South wall:

$$g_2 = T_H - g_1 - g_3 - g_4 \tag{20}$$

Vertical wall:

$$g_1 = T_C - g_2 - g_3 - g_4 \tag{21}$$

3   Code validation

The problem of convection in a triangular cavity has been studied by several authors. The validation of our code is tested first for a Rayleigh number equal to 2772 with the results obtained in references [Asan and Namli (2001); Akinsete and Coleman (1982); Tzeng , Liou and Jou (2005)] by comparing the local Nusselt number (**Fig. 2**). For the case I, The numerical results are found to be good agreement with those of previous studies [Oztop , Varol , Koca and Firat (2012)] **Fig. 3** presents the temperature profiles along the x-axis for several values of y / H, with $Ra = 1.5 \times 10^4$ and Φ=0. In conclusion, the results of this code show good agreement with the published results. This shows that the present LBM code generates very accurate results compared with reference results; moreover the LBM is a reliable tool for the solution of coupled flow and heat transfer.

4   Results and discussion

4.1   *Case I*

In this section, we will study the effect of the variation of the inclination angle and the effect of the variation of the Rayleigh number on temperature distribution inside the aforementioned triangular cavity. For the Rayleigh number, it varies in the range of 1.5×10^3 to 1.5×10^6, while Φ varies in steps of 30° in the range 0° to 120°.

Fig. 4-5 presents respectively, the isotherms and streamlines for several values of Rayleigh number and different inclination angles. The bold isotherm allows us
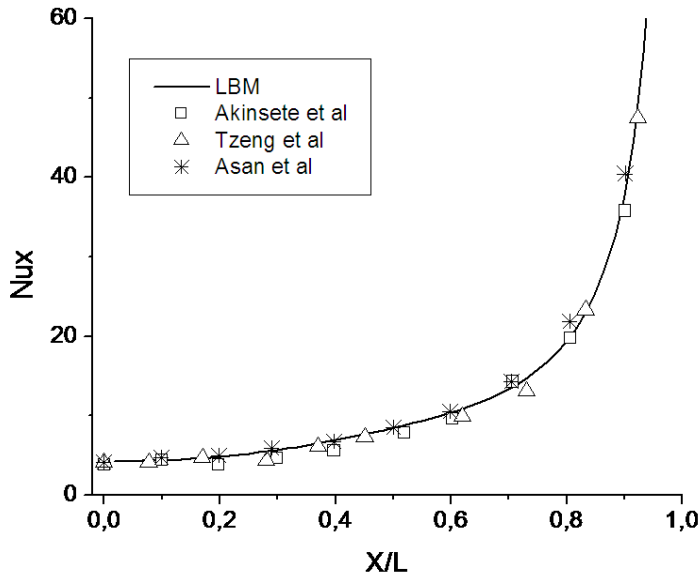
Figure 2: Comparison of numerical results of local Nusselt numbers for triangular geometry with literature

to better monitor the variation of the temperature distribution inside the triangular cavity, this line corresponds to the temperature $\frac{T-T_c}{T_h-T_c} = 0.5$.

For all inclination angles it can be seen that the heat transfer is mainly governed by conduction in the corners of cavity for the values of the Rayleigh number ranging from 1.5×10^3 to 1.5×10^5. These corners are inactive hydrodynamic regions, the flow cannot reach these corners, it appears from the absence of cells in these regions. We note for high Rayleigh number values $(1.5 \times 10^5 \text{and} 1.5 \times 10^6)$, the maximum of the stream function decreases with increasing inclination angle. This decrease with the inclination angle (0 °-120°) means that more fluid velocity decreases and the convection is disadvantaged. This appears clearly in **Fig. 6**, which represents the profile of the velocity components along the y-axis for x / L = 0.5.

4.1.1   Effect of the inclination angle

$\Phi = 0°$, the hot wall is situated at the bottom of the triangle. A single cell is formed; rotating in the clockwise direction, the maximum absolute value of the stream function for $Ra = 1.5 \times 10^6$ is 250 times larger than its value for $Ra = 1.5 \times 10^3$. More Rayleigh number increases, the fluid flow in the cavity increases. Convection is dominant for the high Rayleigh number, which causes the reduction
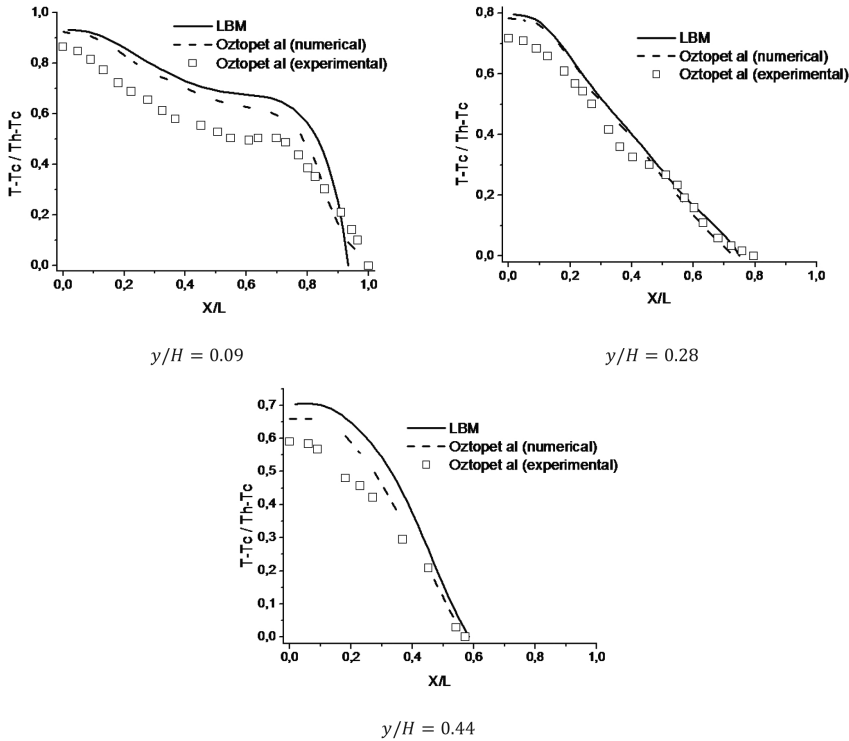
$y/H = 0.09$

$y/H = 0.28$

$y/H = 0.44$

Figure 3: Comparison of local temperature along the x-axis for several values of y / H with experimental and numerical results for $Ra = 1.5 \times 10^4$

of the boundary layer. This decrease in the boundary layer can also be seen by the distribution of isotherms for this angle.

$\Phi = 30°$, a single cell is formed, rotating in the counterclockwise direction; convection is still dominant for high values of Rayleigh number. For $Ra = 1.5 \times 10^6$ we see the appearance of small cells next to the intersection of hot and cold walls, rotating clockwise.

$\Phi = 60°$, the cold wall is situated at the top of the triangular cavity. For small values of Rayleigh number one cell is formed at the center of the cavity, rotating in the anticlockwise direction. For $Ra = 1.5 \times 10^6$, a second cell, of oval shape, is formed close to the adiabatic wall. With increasing Rayleigh number, the fluid is compressed near the walls, and the layer of cold fluid cannot reach the lower part of the cavity. The center of the cavity loses its hydrodynamic effect.

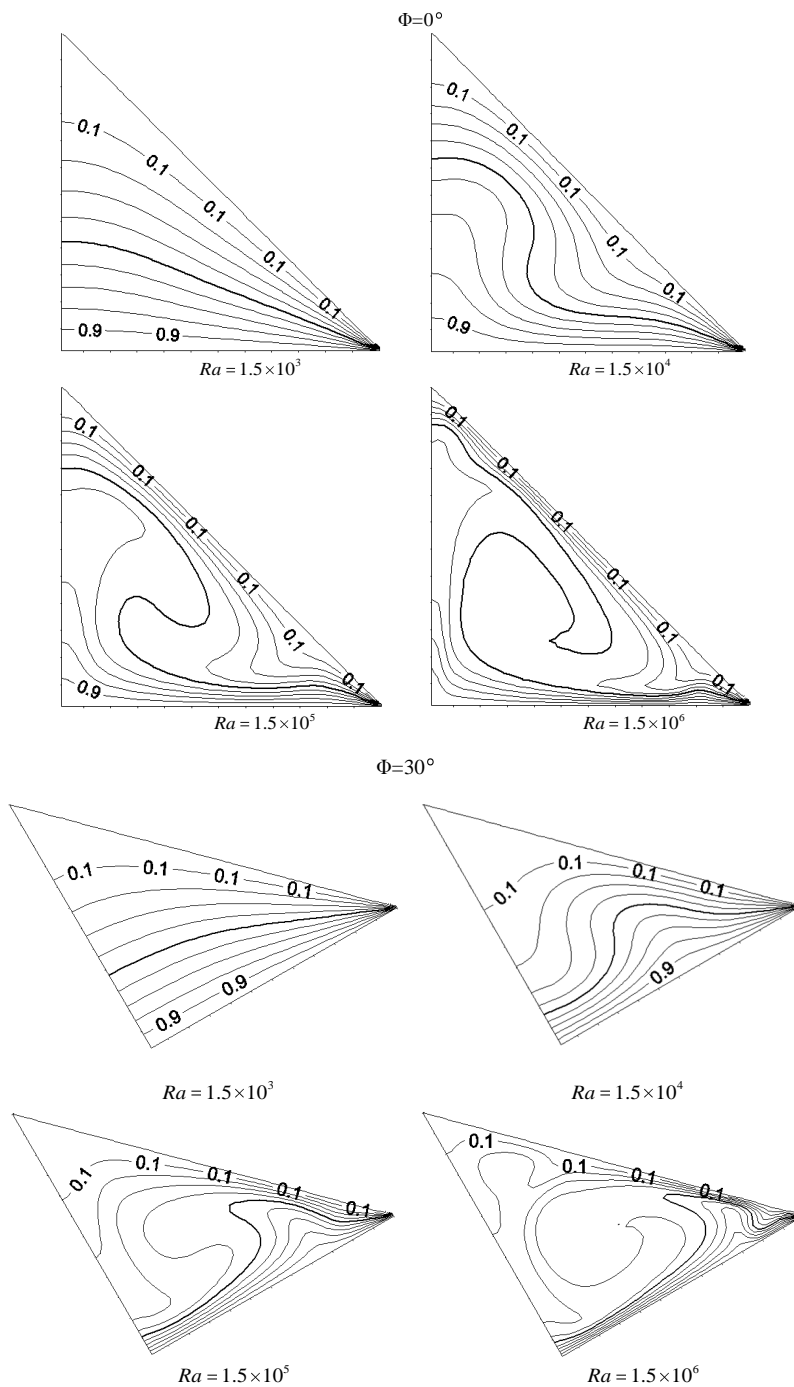$\Phi = 90°$, the hot wall is vertical, the effect of convection is disadvantaged compared

Figure 4: Isotherms for different Rayleigh numbers and for different inclination angle
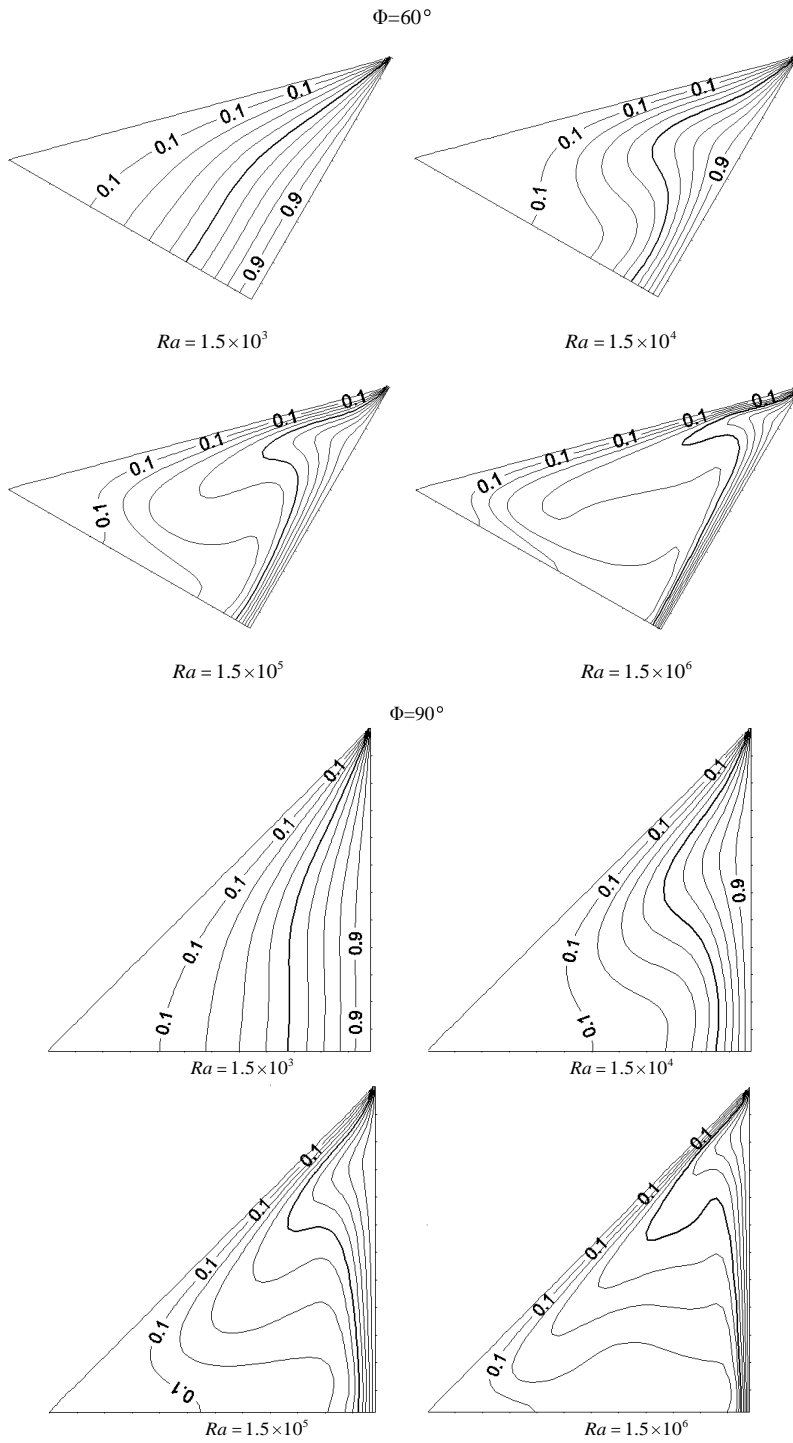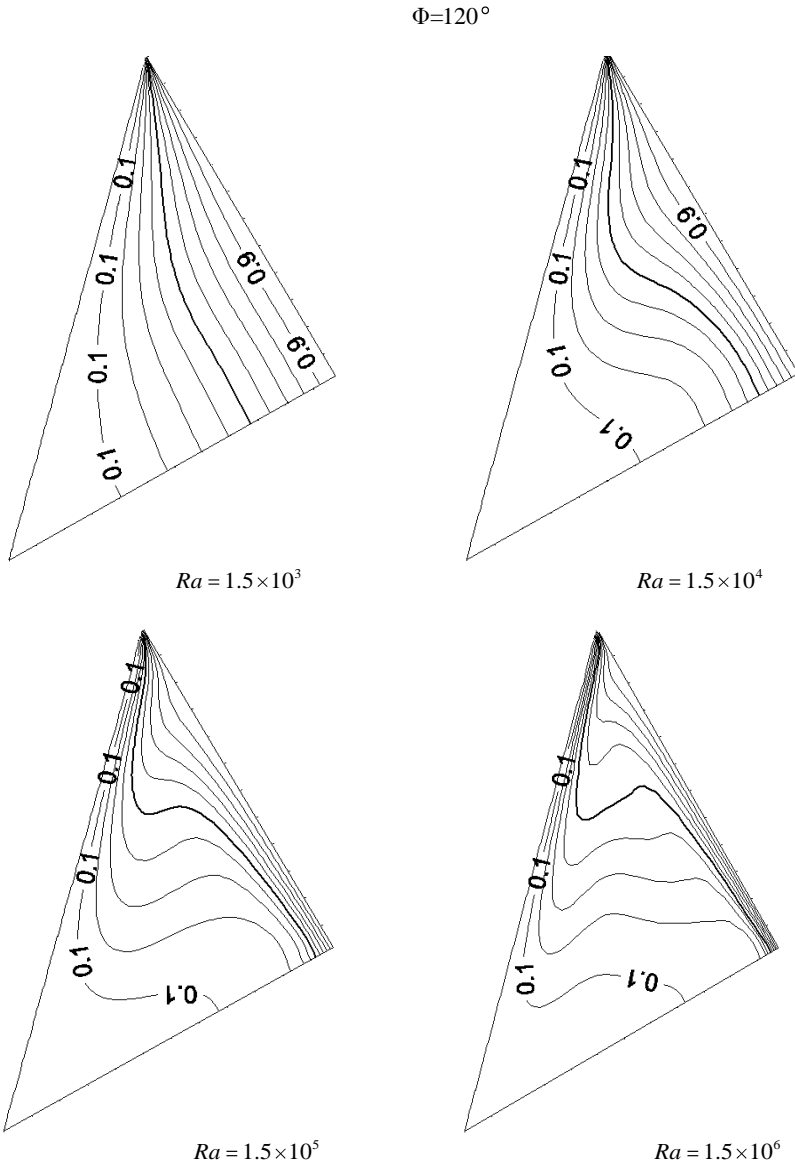
$\Phi=60°$

$Ra = 1.5 \times 10^3$ $Ra = 1.5 \times 10^4$

$Ra = 1.5 \times 10^5$ $Ra = 1.5 \times 10^6$

$\Phi=90°$

$Ra = 1.5 \times 10^3$ $Ra = 1.5 \times 10^4$

$Ra = 1.5 \times 10^5$ $Ra = 1.5 \times 10^6$

Figure 4: (continued)

$\Phi=120^{\circ}$

$Ra = 1.5 \times 10^{3}$

$Ra = 1.5 \times 10^{4}$

$Ra = 1.5 \times 10^{5}$

$Ra = 1.5 \times 10^{6}$

Figure 4: (continued)
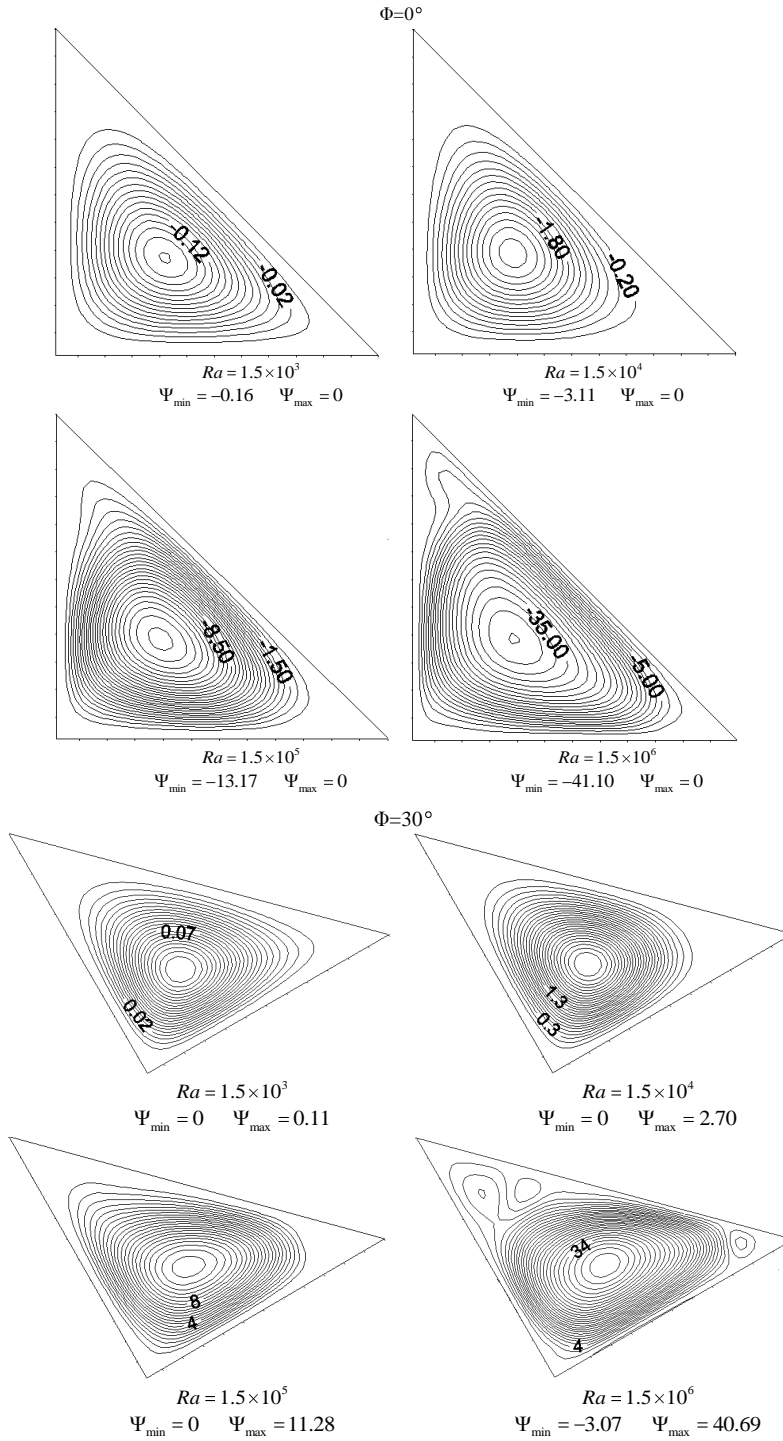
Figure 5: Streamlines for different Rayleigh numbers and for different inclination angle

$\Phi = 60°$

$Ra = 1.5 \times 10^3$	$Ra = 1.5 \times 10^4$
$\Psi_{min} = 0 \quad \Psi_{max} = 0.33$	$\Psi_{min} = 0 \quad \Psi_{max} = 3.15$
$Ra = 1.5 \times 10^5$	$Ra = 1.5 \times 10^6$
$\Psi_{min} = 0 \quad \Psi_{max} = 10.42$	$\Psi_{min} = 0 \quad \Psi_{max} = 22.09$

$\Phi = 90°$

$Ra = 1.5 \times 10^3$	$Ra = 1.5 \times 10^4$
$\Psi_{min} = 0 \quad \Psi_{max} = 0.43$	$\Psi_{min} = 0 \quad \Psi_{max} = 2.99$
$Ra = 1.5 \times 10^5$	$Ra = 1.5 \times 10^6$
$\Psi_{min} = 0 \quad \Psi_{max} = 8.38$	$\Psi_{min} = 0 \quad \Psi_{max} = 16.37$

Figure 5: (continued)

Φ=120°

$Ra = 1.5 \times 10^3$
$\Psi_{min} = 0$ $\Psi_{max} = 0.41$

$Ra = 1.5 \times 10^4$
$\Psi_{min} = 0$ $\Psi_{max} = 2.40$

$Ra = 1.5 \times 10^5$
$\Psi_{min} = 0$ $\Psi_{max} = 6.61$

$Ra = 1.5 \times 10^6$
$\Psi_{min} = 0$ $\Psi_{max} = 13.24$

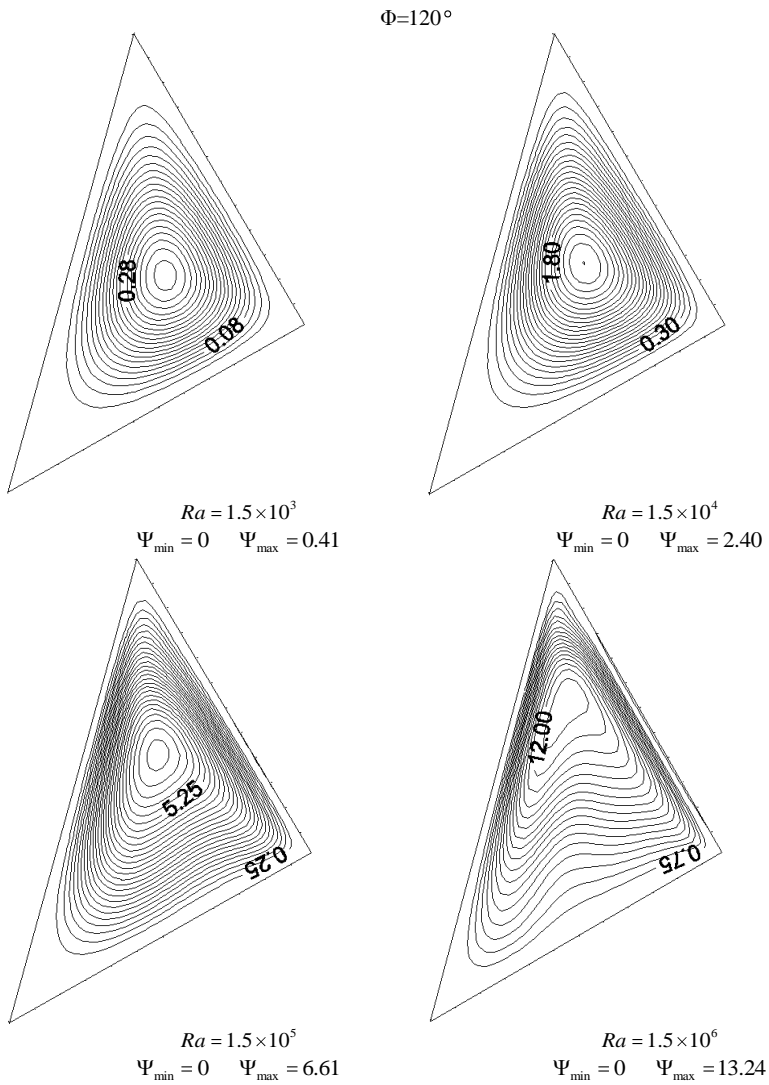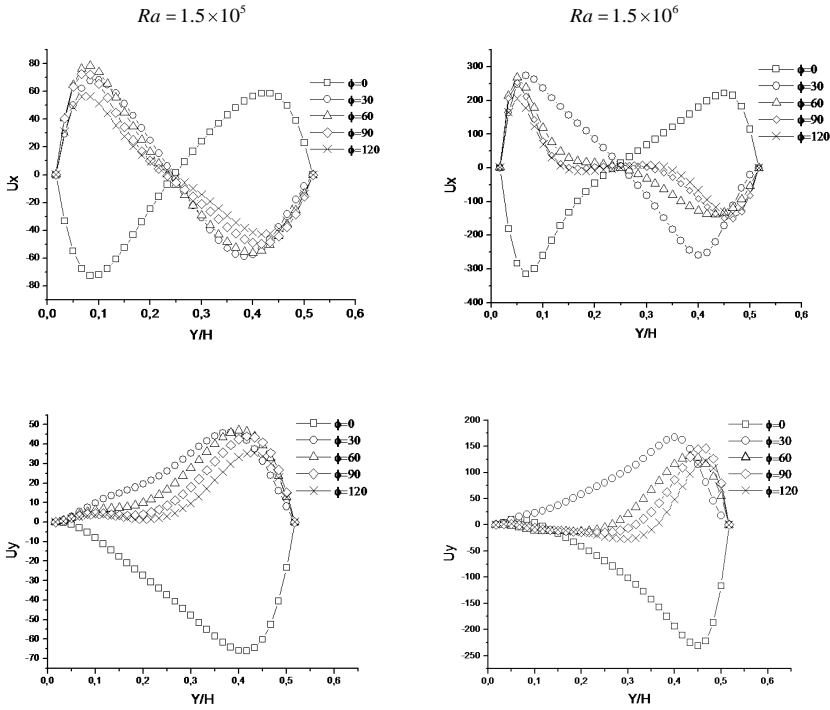Figure 5: (continued)

$$Ra = 1.5 \times 10^5 \qquad\qquad Ra = 1.5 \times 10^6$$
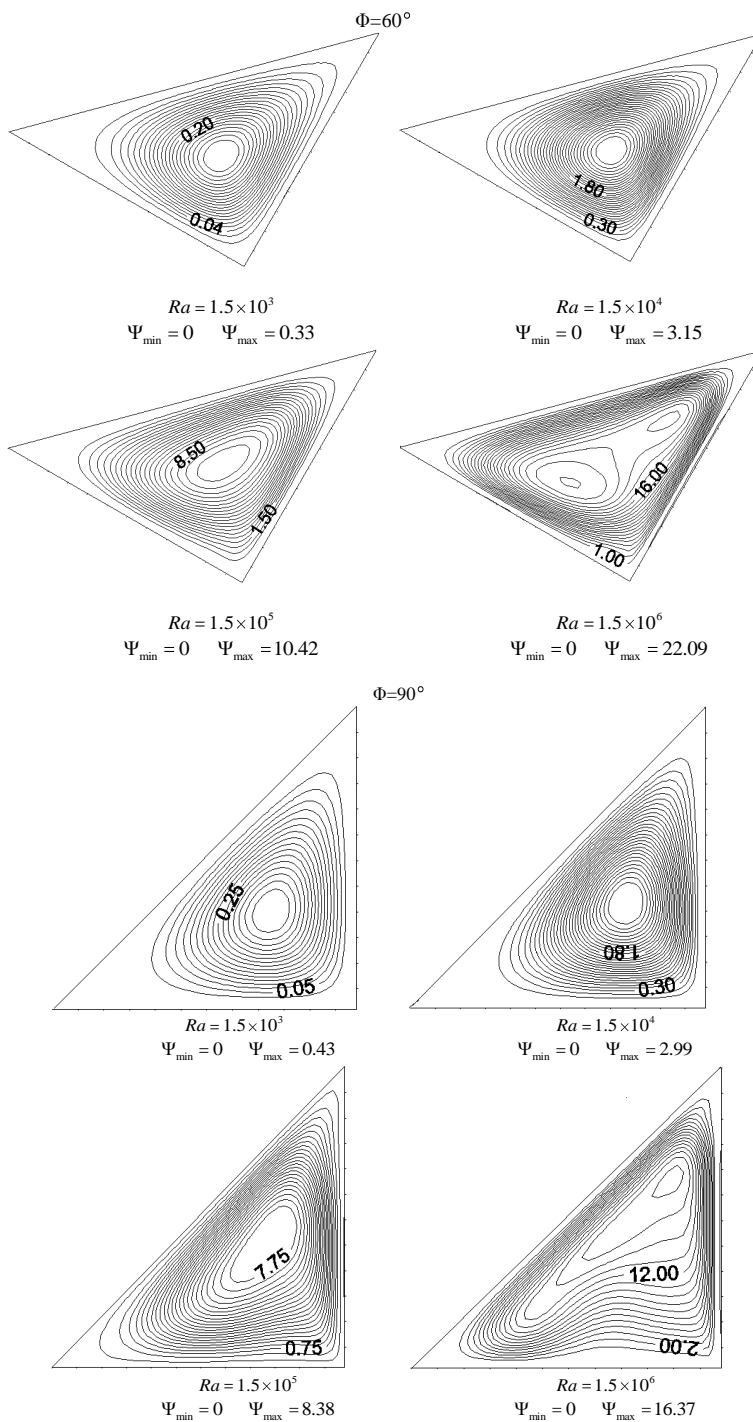
Figure 6: Variation along the y-axis of the velocity components for x/L=0.5 for several Rayleigh number
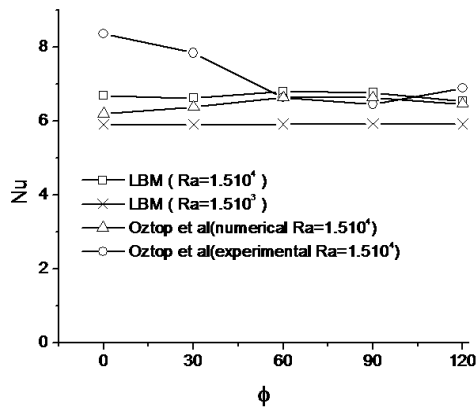
Figure 7: Variation of Nuselt number as function of the inclination angle for different Rayleigh number

to the case $\Phi = 0°$, a single cell is formed to rotate in the anticlockwise direction. As the more the Rayleigh number increases, the more the center of its cell moves to the point of intersection of the hot and cold walls. In addition the fluid flow becomes increasingly tight on the hot and cold walls.

$\Phi = 120°$, a single cell is formed to rotate in the anticlockwise direction. The more the Rayleigh number increases, the more the center of its cell moves to the point of intersection of the hot and cold walls. For the range of angles in this case study, $\Phi = 120°$ corresponds to the angle at which the convection is more disadvantaged. This becomes clear by the low velocity of flow (**Fig. 6**), as by the minimum value average Nusselt number (**Fig. 7**).

Fig. 7 shows the variation in average Nusselt number by varying the inclination angle. For Ra = 1.5×10^4, the experimental results obtained by reference [Oztop, Varol, Koca and Firat (2012)] clearly show that the increase of the tilt angle causes the decrease of Nusselt number, it means that convection is more disadvantaged.

4.2   *Case II*

In this section we will discuss the variation of the temperature distribution in the cavity with the boundary conditions already cited in **Table 1**, by varying the Rayleigh number and by varying the inclination angle. The Rayleigh number varies in the range of 10^3 to 10^6, for a tilt angle varied from 0° to 360°. **Fig. 8-9** presents respectively, the isotherms and streamlines for several values of Rayleigh number and different inclination angles. The bold isotherm allows us to better monitor the variation of the temperature distribution inside the triangular cavity, this line corresponds to the temperature $\frac{T - T_c}{T_h - T_c} = 0.5$

4.2.1   *Effect of the inclination angle*

$\Phi = 0°$ When increasing the Rayleigh number convection is favored. For values of Rayleigh number above 10^5 convection is dominant, the maximum value of the stream function, for the Rayleigh number equal to 10^6, is 150 times as larger as its value when the Rayleigh is equal to 10^3. Fluid flow within the cavity is more intense for the high values of Rayleigh; this causes the reduction of the thickness of boundary layer which is shown clearly in the isotherms.

$\Phi = 90°$ the lower side of the triangle is cold, the heat transfer is mainly by conduction even for large values of the Rayleigh number, this appears by the low values of the stream function and also by the distribution of temperature which is maintained unchanged for the value of the Rayleigh number equal to 10^5. This means that the heat transfer is not controlled by convection. The fluid is stratified near the cold wall and we are in dominated conducting regime.
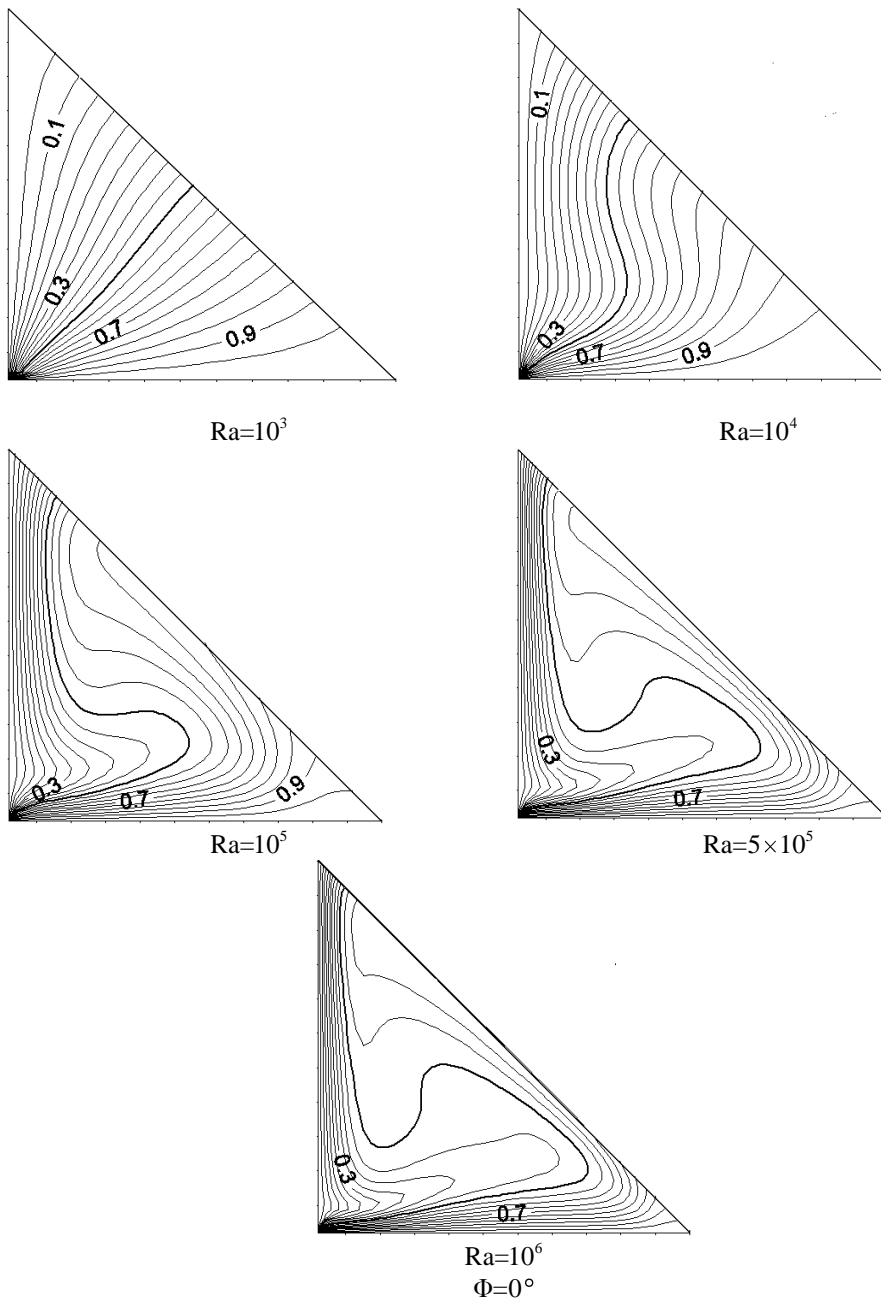
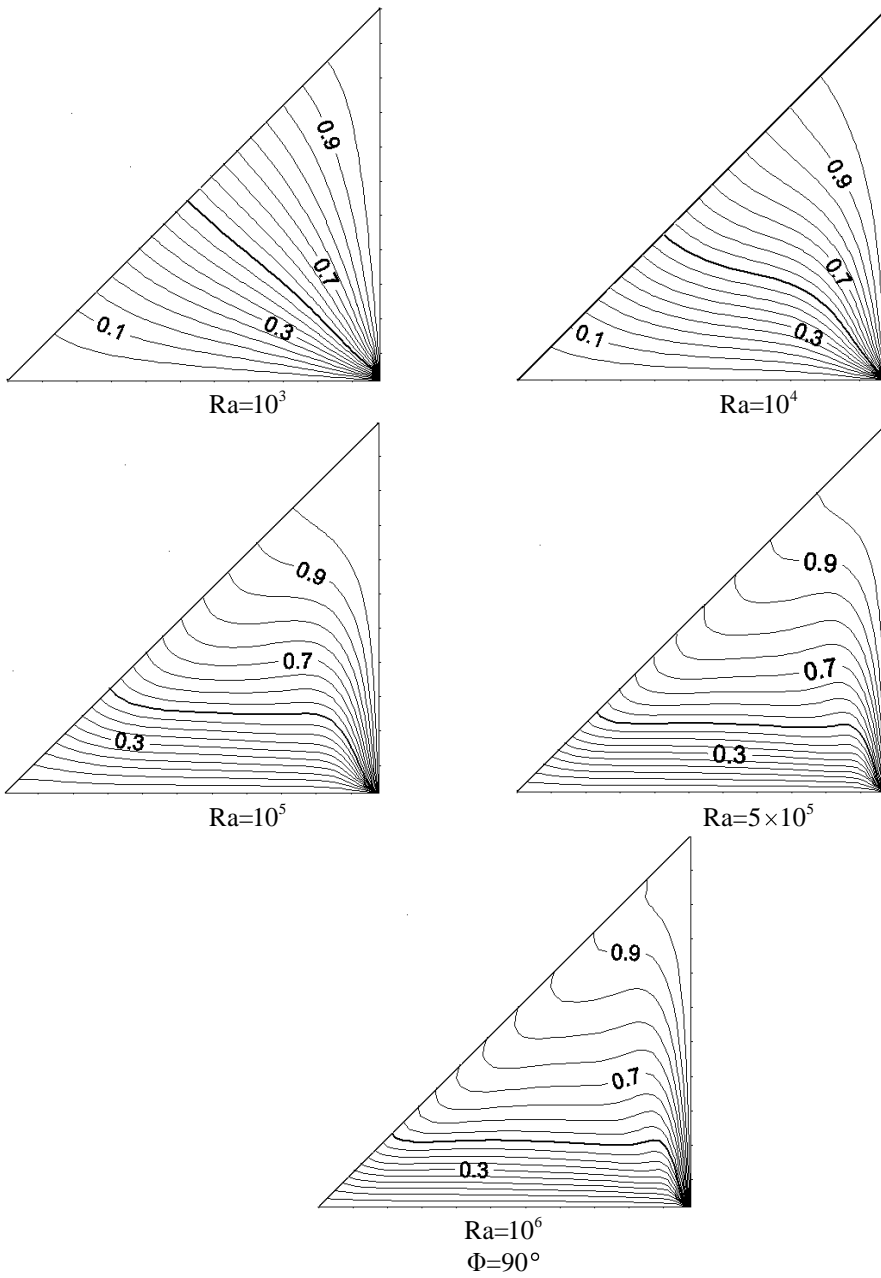Figure 8: Isotherms for different Rayleigh numbers and for different inclination angle
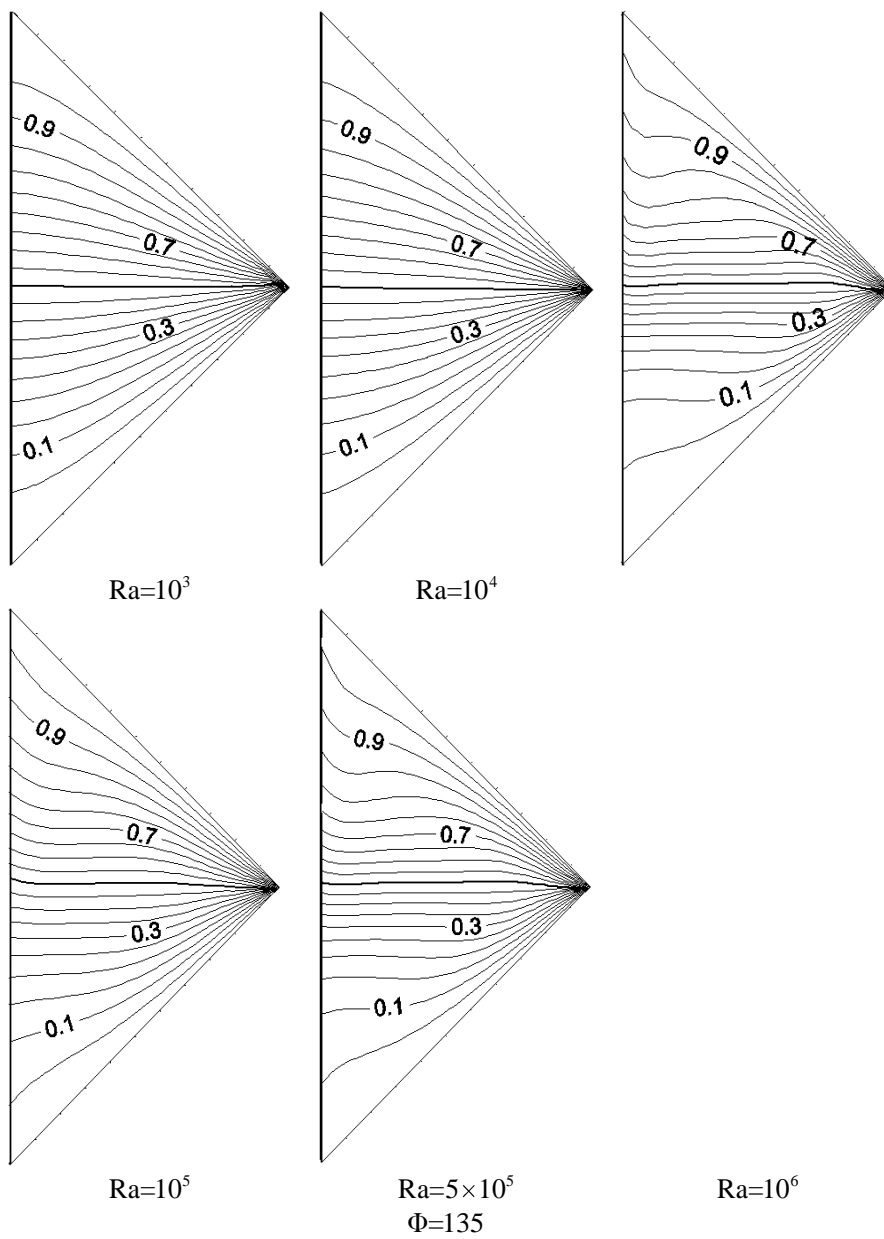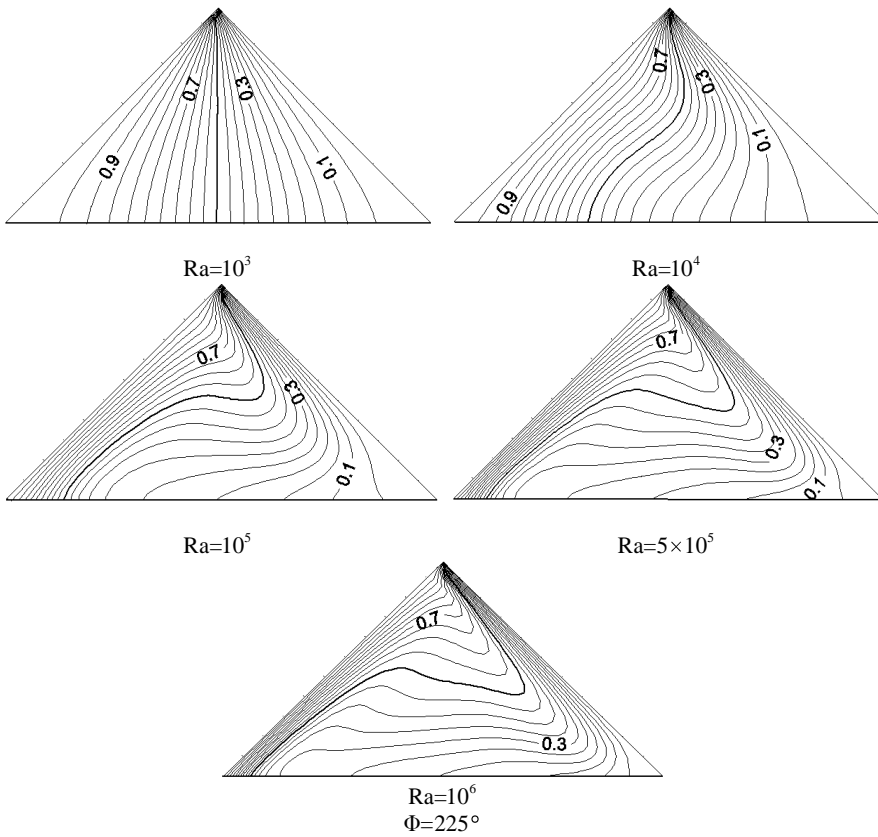
Figure 8: (continued)

Ra=10^3 Ra=10^4

Ra=10^5 Ra=5×10^5 Ra=10^6
Φ=135

Figure 8: (continued)

Ra=10^3

Ra=10^4

Ra=10^5

Ra=5×10^5

Ra=10^6
Φ=225°

Figure 8: (continued)

Ra=10³

Ra=10⁴

Ra=10⁵

Ra=5×10⁵

Ra=10⁶
Φ=270°

Figure 8: (continued)

Ra=10^3 Ra=10^4

Ra=10^5 Ra=5×10^5 Ra=10^6
                   $\Phi=315°$
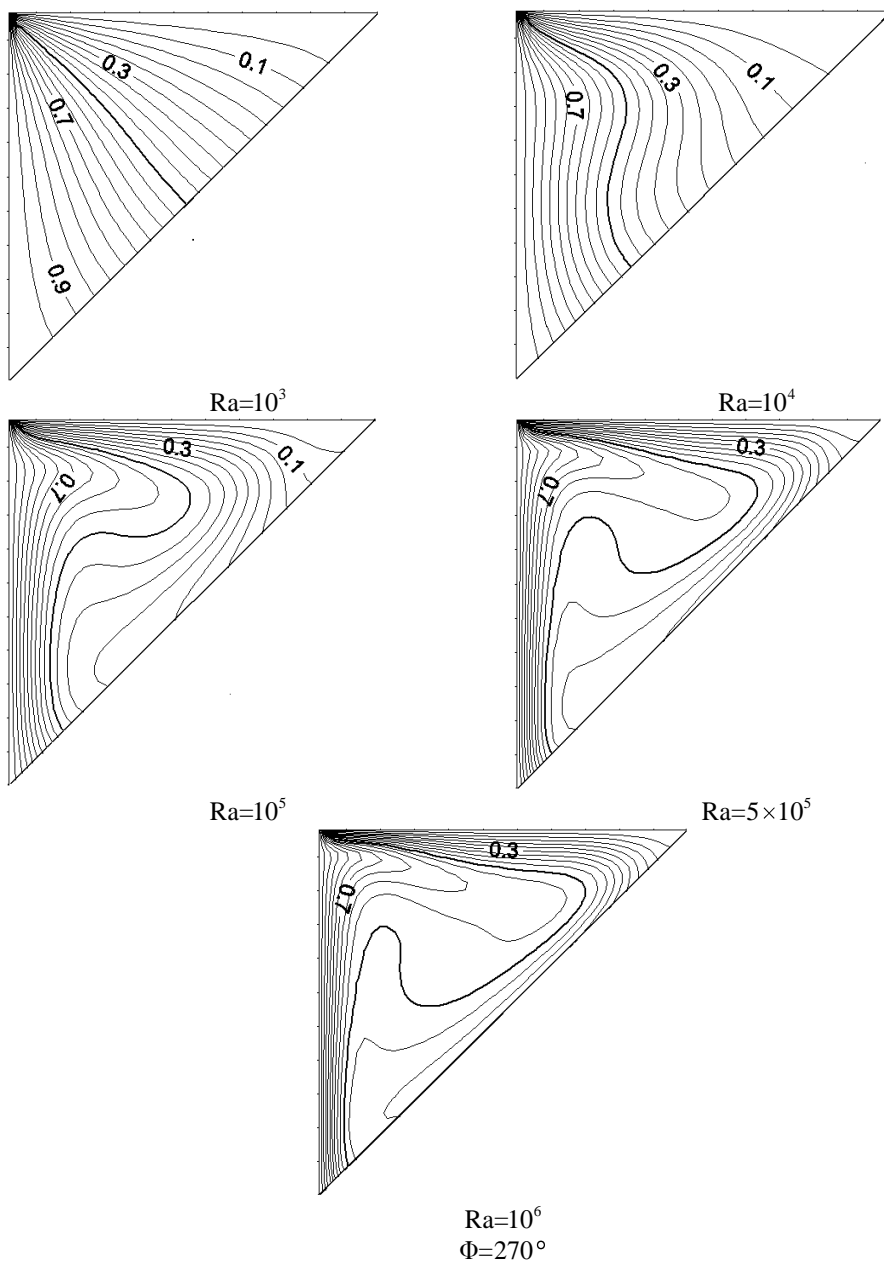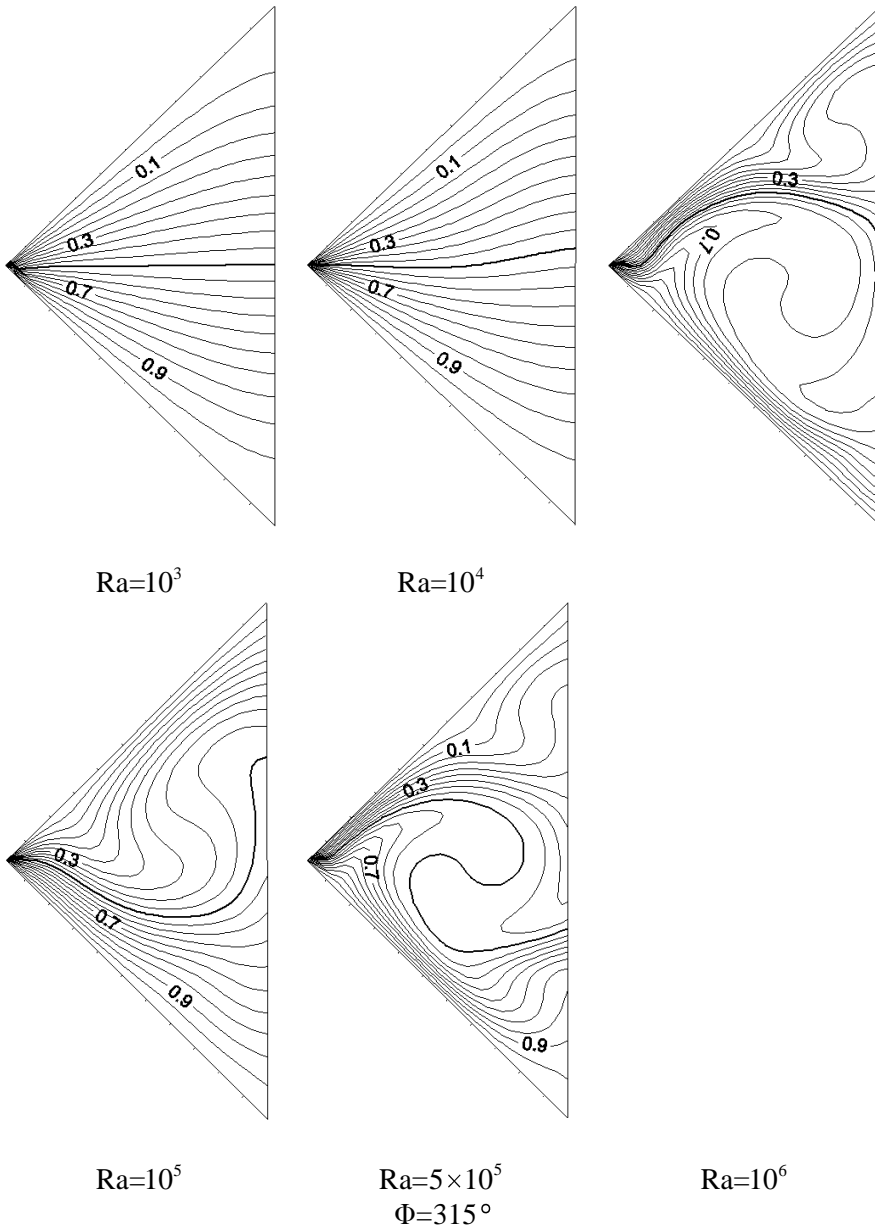
Figure 8: (continued)
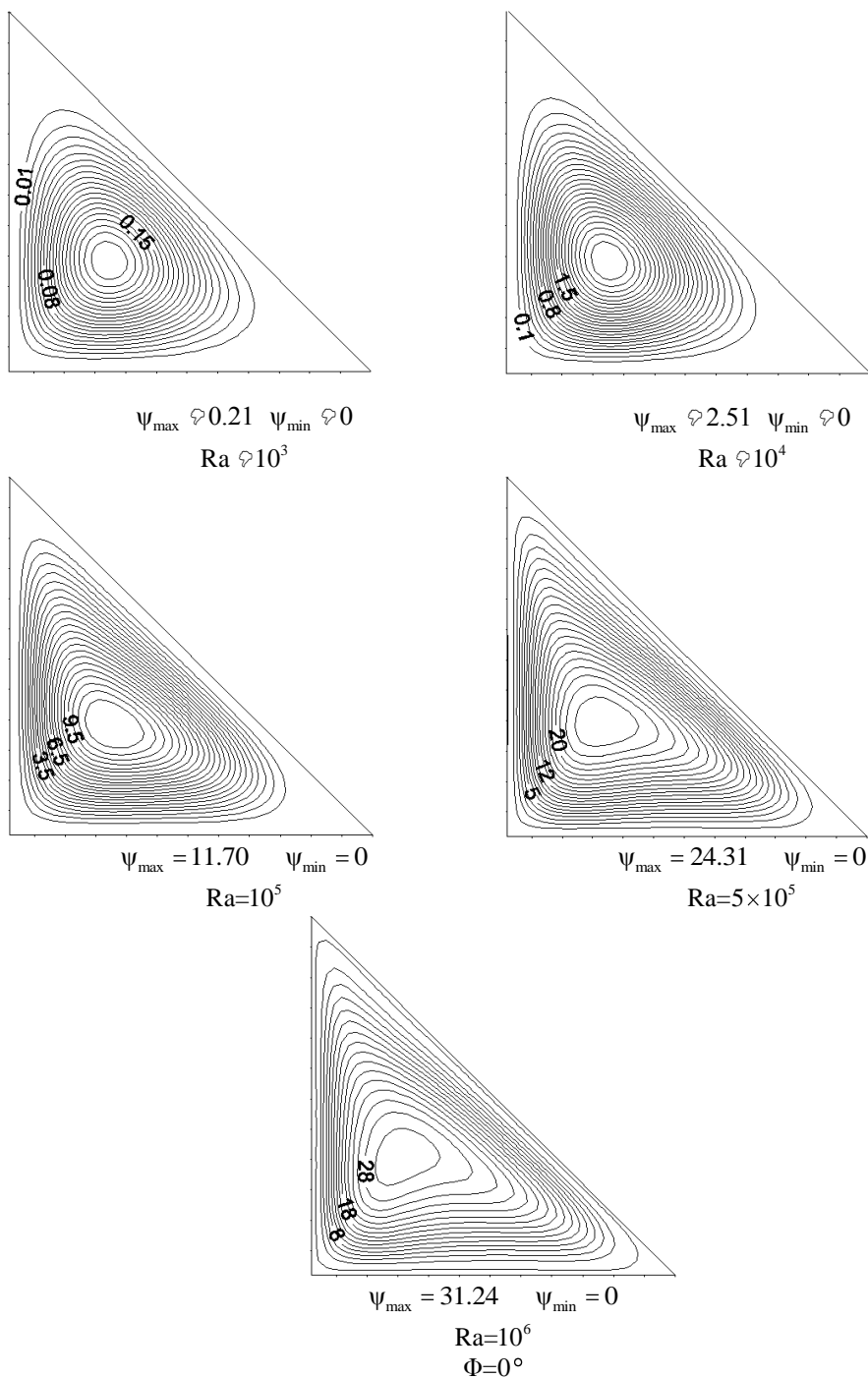
Figure 9: Streamlines for different Rayleigh numbers and for different inclination angle

$\psi_{max} = 0.18$ $\psi_{min} = 0$

Ra=10^3

$\psi_{max} = 1.19$ $\psi_{min} = 0$

Ra=10^4

$\psi_{max} = 3.69$ $\psi_{min} = 0$

Ra=10^5

$\psi_{max} = 6.11$ $\psi_{min} = 0$

Ra=5×10^5

$\psi_{max} = 7.81$ $\psi_{min} = 0$

Ra=10^6

Φ=90°

Figure 9: (continued)

$\psi_{max} = 0.024$ $\psi_{min} = -0.023$
Ra=10³

$\psi_{max} = 0.22$ $\psi_{min} = -0.18$
Ra=10⁴

$\psi_{max} = 5.71$ $\psi_{min} = -2.74$

$\psi_{max} = 1.70$ $\psi_{min} = -1$

Ra=10⁵

$\psi_{max} = 3.91$ $\psi_{min} = -2.14$

Ra=5×10⁵
Φ=135°

Ra=10⁶
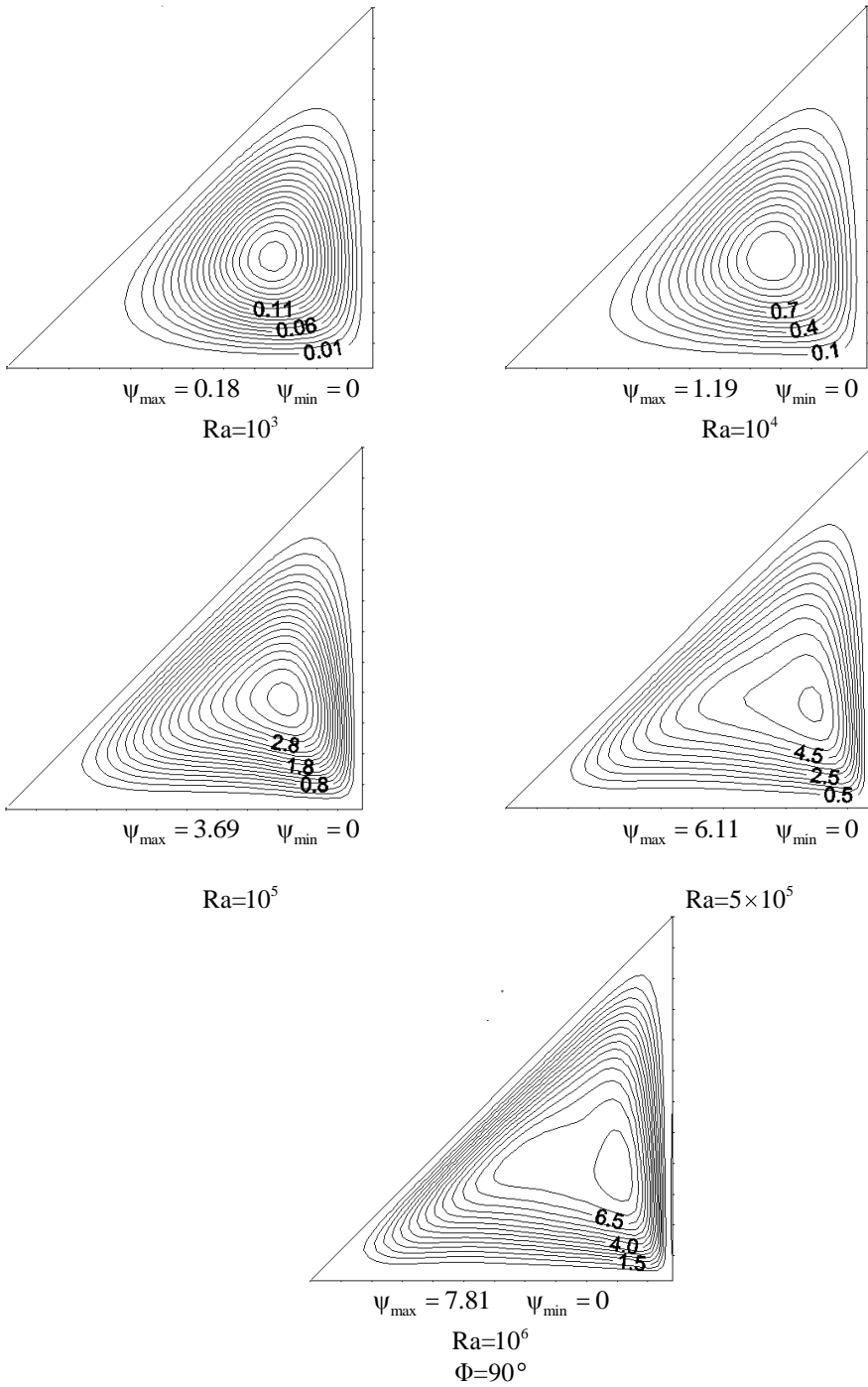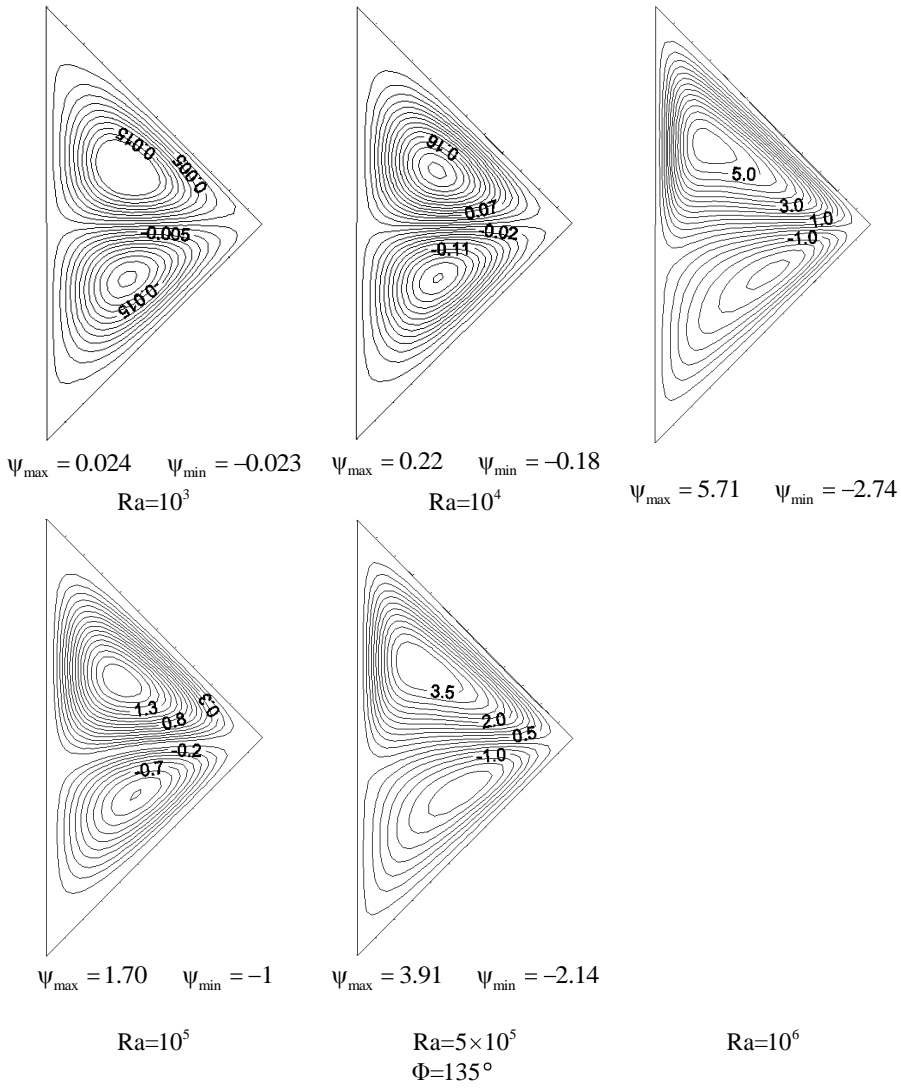
Figure 9: (continued)

Figure 9: (continued)

$\psi_{max} = 0 \qquad \psi_{min} = -0.20$
$Ra=10^3$

$\psi_{max} = 0 \qquad \psi_{min} = -2.48$
$Ra=10^4$

$\psi_{max} = 0 \qquad \psi_{min} = -11.86$
$Ra=10^5$

$\psi_{max} = 0 \qquad \psi_{min} = -25.14$
$Ra=5\times10^5$

$\psi_{max} = 0 \qquad \psi_{min} = -32.38$
$Ra=10^6$
$\Phi=270°$

Figure 9: (continued)

$\psi_{max} = 0.026 \quad \psi_{min} = -0.023$ $\psi_{max} = 0.44 \quad \psi_{min} = -0.13$

Ra=10^3 Ra=10^4 $\psi_{max} = 11.25 \quad \psi_{min} = -32.28$

$\psi_{max} = 8.60 \quad \psi_{min} = -1.2$ $\psi_{max} = 5 \quad \psi_{min} = -21.22$

Ra=10^5 Ra=5×10^5 Ra=10^6
                                   $\Phi = 315°$
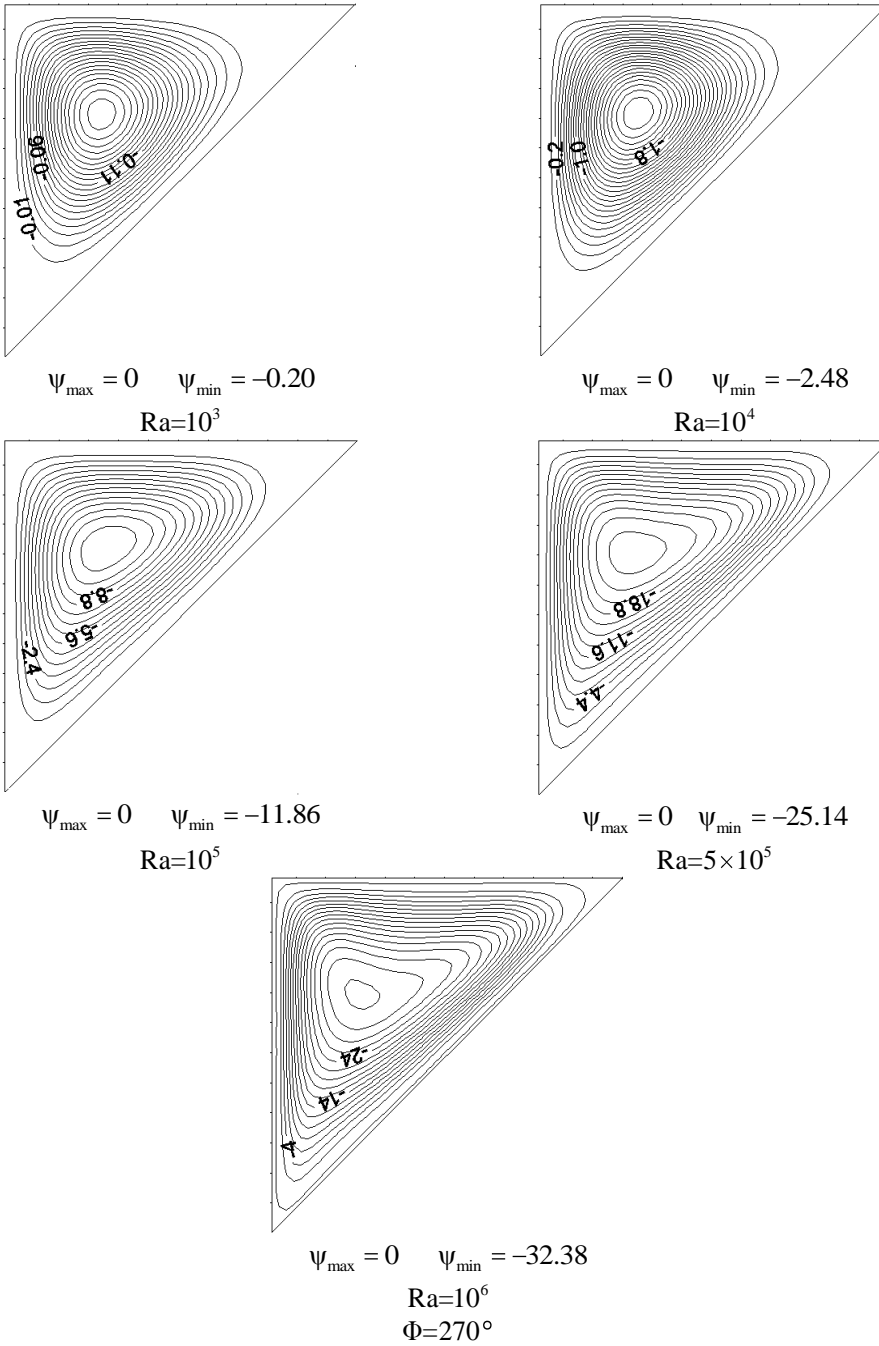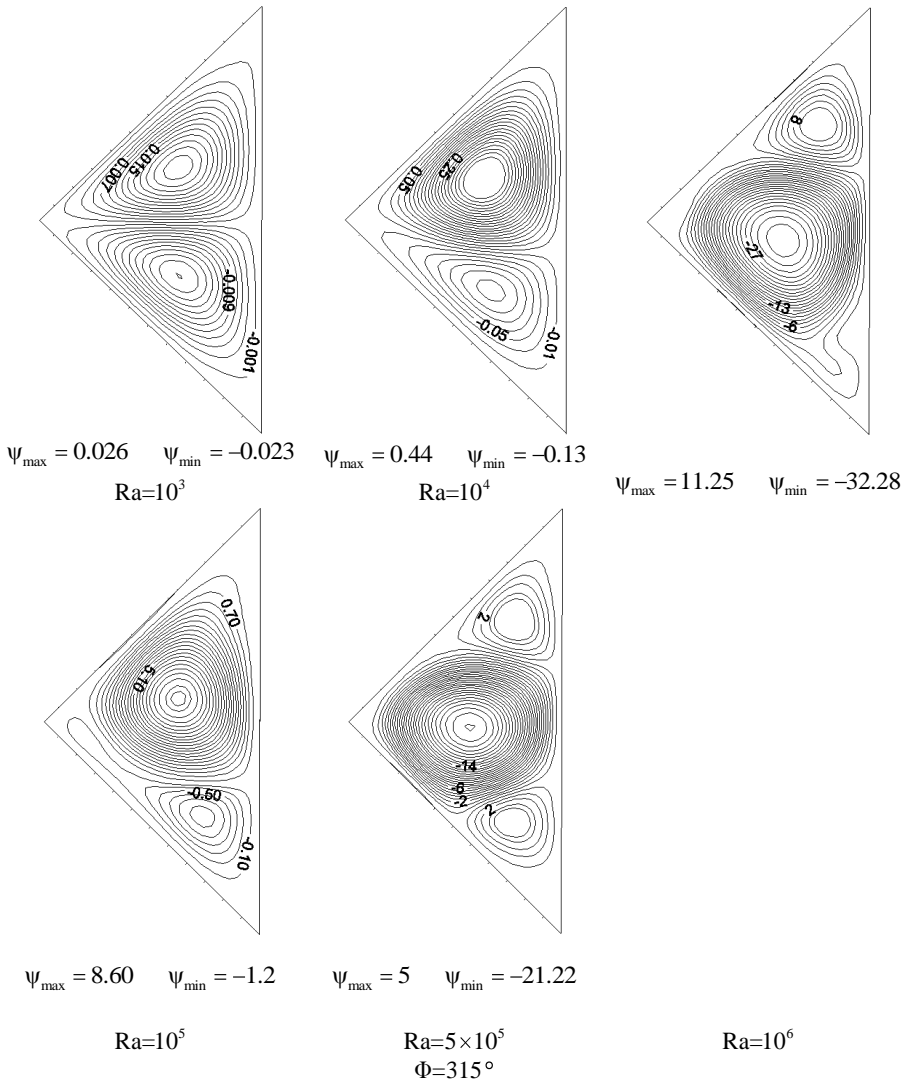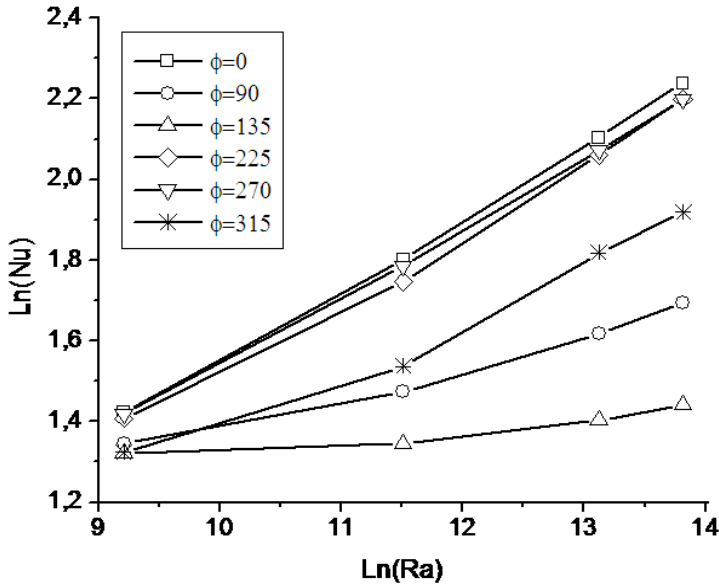
Figure 9: (continued)

Figure 10: Average Nusselt number on the heated wall versus Rayleigh number

$\Phi = 135°$ Two contra-rotating cells are formed inside the cavity for all values of Rayleigh number, the top cell is rotating counterclockwise and the lower cell is rotating in the clockwise. The two cells are not symmetrical. The velocity intensity next to hot wall is higher than the velocity intensity next to the cold wall. The inclined lower side is cold. The inclined upper side is hot, the heat transfer is mainly by conduction even for large values of the Rayleigh number, and it appears by the low values of the stream function even for large values of the Rayleigh number.

$\Phi = 225°$ a single cell is formed rotating in the clockwise direction, the increase of Rayleigh number favors convection. For values higher than 10^5 convection is dominant, the fluid flow within the cavity is stronger for large values of Rayleigh. This causes the reduction of the boundary layer.

$\Phi = 270°$ the upper side is cold, the hot side is vertical, this implies that the heat transfer by convection is very intense for this angle. A single cell is formed by rotation in the clockwise direction. The more the value of the Rayleigh number increases, the more the convection is more dominant and the boundary layer becomes thinner.

$\Phi = 315°$ the hot wall is at the bottom and the cold wall is at the top of the cavity. For the Rayleigh number equal to 10^3, the conduction is dominant. Two symmetric

contra rotating cells are formed. The bottom cell is rotating clockwise and the top cell is rotating in a counterclockwise direction. The temperature distribution inside of the cavity is symmetrical. When increasing the Rayleigh number the convection regime is favored and the cells symmetry is broken. For the Rayleigh number equal to 10^5, two contra-rotating cells are formed; the largest one is situated on the upper zone of the domain and is rotating counterclockwise, the small cell is at the bottom and rotating in the opposite direction. The hole of the cavity is cold. The effect of convection has not the required power for heating the entire cavity. For the Rayleigh number equal to 5×10^5 three cells are formed, the larger cell is in the middle of the cavity and is rotating in the clockwise direction, and the temperature is uniform in the middle of the cavity. For the Rayleigh number equal to 10^6, two contra rotating cells are formed; the largest cell is on the bottom of the cavity rotating in the clockwise direction the small cell is at the upper of the cavity and is rotating on the opposite direction. The effect of convection becomes very intense, and the majority of the cavity is heated.

Fig. 10 shows the variation of the Nusselt number as function of the Rayleigh number for several inclination angles. Convection is dominant and the value of the Nusselt number increases with increasing Rayleigh number. For angles $\Phi = 90°$ and $135°$ conduction is dominant, and the Nusselt number is in its minimum value compared to other angles. The highest values of the Nusselt number obtained for $\Phi = 0°$, $270°$ and $225°$ where convection is dominant. In addition to Rayleigh number, it is clear that the inclination angle is a controlling parameter of heat transfer in the cavity.

5   Conclusion

In this work we have assessed the ability of the so-called double-population Lattice Boltzmann Method for the study of free convection in a right-angled triangular cavity. We have considered a Rayleigh number spanning the range 10^3 to 10^6 and an inclination angle varying from $0°$ to $120°$ for case I (adiabatic vertical wall and inclined isothermal wall) and from $0°$ to $360°$ for case II (isothermal vertical wall and adiabatic inclined wall).

- For both cases, an increase in the Rayleigh number strengthens both fluid flow and the heat transfer rate.

- For Case I and Ra=10^3, the heat transfer rate does not depend on the inclination angle.

- For Case I and Ra>10^3, an increase in the inclination angle from $0°$ to $120°$ tends to mitigate the fluid flow and the heat transfer rate.

- For Case II, and over the entire range of values of the Rayleigh number considered, heat transfer is favoured for $\Phi = 0°$, $225°$ and $270°$ (convection is stronger); in particular, the best heat transfer rate is attained for $\Phi = 0°$.

- For Case II, and over the entire range of values of the Rayleigh number considered, the lowest heat transfer rate is obtained for $\Phi = 135°$ (for this value of Φsgonvection is significantly weakened).

References

Akinsete, V.; Coleman, T. A. (1982): Heat transfer by steady laminar free convection in triangular enclosures. *Int. J. Heat Mass Transfer.* vol.25, pp.991-998.

Asan, H.; Namli, L. (2001): Numerical simulation of buoyant flow in a roof of triangular cross section under winter day boundary conditions. *Energy Buildings,* vol.33, pp.753-757.

Basak, T.; Anandalakshmi, R.; Gunda, P. (2012): Role of entropy generation during convective thermal processing in right-angled triangular enclosures with various wall heatings. *Chemical Engineering Research and Design,* vol.90, pp.1779-1799.

Benzi, R.; Succi, S.; Vergassola, M. (1992): The lattice Boltzmann equation: theory and applications. *Phys. Rep.,* vol. 222, pp.145–197.

Catton, I. (1978): Natural convection in enclosures, Proc. 6th Int. *Heat Transfer Conf.* vol.6, pp.13–31.

Chen, S.; Doolen, G. D. (1998): Lattice Boltzmann method for fluid flows. *Annual Review of Fluid Mechanics,* vol. 30, pp. 329–64.

Ching, Y. C.; Oztop, H. F.; Rahman, M. M.; Islam, M. R.; Ahsan, A. (2012): Finite element simulation of mixed convection heat and mass transfer in a right triangular enclosure. *Int. Commun. Heat Mass Transfer.* vol.39, pp.689-696.

De Vahl Davis, G. (1983): Natural convection of air in a square cavity: a bench mark numerical solution. *Int. J. Numer. Methods in Fluids,* vol.3, pp.249–264.

Dixit, H. N.; Bab, V. (2006): Simulation of high Rayleigh number natural convection in a square cavity using the lattice Boltzmann method. *Int. J. Heat Mass Transfer,* vol.49, pp.727-39.

Gebhart, B.; Jaluria, Y.; Mahajan, R. P.; Sammakia, B. (1988) *Buoyancy-induced Flows and Transport,* Hemisphere, Washington.

Ghasemi, B.; Aminossadati, S. M. (2010): Mixed convection in a lid-driven triangular enclosure filled with nanofluids. *Int. Commun. Heat Mass Transfer.* vol.37, pp.1142-1148.

Gurkan, Y.; Orhan, A. (2013): Laminar natural convection in right-angled triangular enclosures heated and cooled on adjacent walls. textitInt. J. Heat Mass Transfer. vol.60, pp.365–374.

Higuera, F. J.; Succi, S.; Benzi, R. (1989): Lattice gas dynamics with enhanced collisions. *Europhys. Lett.* vol.9, pp.345–349.

Koca, A.; Oztop, H. F.; Varol, Y. (2007): The effects of Prandtl number on natural convection in triangular enclosures with localized heating from below. *Int. Commun. Heat Mass Transfer,* vol.34, pp.511–519.

Mahmoudi, A. H.; Pop, I.; Shahi, M. (2012): Effect of magnetic field on natural convection in a triangular enclosure filled with nanofluid. *Int. J. Thermal Sciences.* vol.59, pp.126-140.

McNamara, G.; Alder, B. (1993): Analysis of the lattice Boltzmann treatment of hydrodynamic. *Physica A: Statistical Mechanics and its Applications.* vol. 194, pp. 218–28.

Omri, A. (2007): Numerical investigation on optimization of a solar distiller dimensions. *Desalination,* vol.206, pp.373–379.

Ostrach, S. (1988): Natural convection in enclosures. *J. Heat Transfer.* vol.110, pp. 1175–1190.

Oztop, H. F.; Varol, Y.; Koca, A.; Firat, M. (2012): Experimental and numerical analysis of buoyancy-induced flow in inclined triangular enclosures. *Int. Commun. Heat Mass Transfer,* vol.39, pp.1237–1244.

Patankar, S. V. (1980): *Numerical Heat Transfer and Fluid Flow,* Hemisphere, Washington, D.C.

Rahman, M.M., Billah, M.M., Rahman, A.T.M.M., Kalam, M.A., Ahsan, A. (2011): Numerical investigation of heat transfer enhancement of nanofluids in an inclined lid-driven triangular enclosure. *Int. Commun. Heat Mass Transfer,* vol.38, pp.1360–1367.

Succi, S. (2001): The Lattice Boltzmann Equation for Fluid Dynamics and Beyond. Oxford University Press.

Tzeng, S. C., Liou, J. H., Jou, R. Y. (2005): Numerical simulation-aided parametric analysis of natural convection in a roof of triangular enclosures. *Heat Transfer Engineering.* vol.26, pp. 69-79.

Varol, Y. (2011): Natural convection in porous triangular enclosure with a centered conducting body. *Int. Commun. Heat Mass Transfer,* vol.38, pp.368-376.